Free-free transitions in a bichromatic field of frequencies ω and 2ω at moderate field intensities

Aurelia Cionga and Gabriela Zloh

Institute for Space Sciences, P.O. Box MG-36,

Bucharest-Măgurele,Bucharest, R-76900 Romania

Abstract

Free-free transitions in laser-assisted electron-hydrogen scattering in a bichromatic field of frequencies ω and 2ω are studied at moderate intensities for fast projectiles. A hybrid approach is used, in which the field-projectile interaction is described exactly but the field-target one is described by second order perturbation theory; the projectile-target interaction is treated in the first Born approximation. The adopted description of the target enables a consistent study of the leading process to each of the considered sidebands. Numerical results are presented for the angular distributions in a geometry and at frequencies for which the target dressing is important. The influence of the relative phase between the fields is investigated, too.

Keywords:

I. INTRODUCTION

In the last years it has been observed that laser-assisted and laser-induced processes may be considerably modify when they take place in a bichromatic field. In this context, a special attention is shown to the case of commensurate frequencies, in connection with high harmonic generation experiments. Theoretical investigations on free-free transitions in laser-assisted electron-atom scattering in a bichromatic field have recently been published. We quote here the paper by Varró and Ehlotzky [1], where the development of the topic is presented. The early results were obtained for low frequencies, neglecting the dressing of the target [2]. They represent generalizations of the Bunkin and Fedorov formula [3], but there are results [4] which go beyond the first Born approximation in the scattering potential, extending the Kroll-Watson formula [5] to a bichromatic field. However, perturbative calculations for both monochromatic [6]-[7] and bichromatic fields [8] have shown that the dressing of the target by the radiation field plays an important role when the field frequency is no longer small. Varró and Ehlotzky [1] were the first to take into account the effect of target dressing in free-free transitions in a bichromatic field at moderate field intensities for fast projectiles. They extend the approach introduced by Byron and Joachain [9] to deal with the same problem in the monochromatic case. In this treatment the interaction between the projectile and the field is the only one to be treated exactly; the other two, namely the interaction between the field and the bound electron and the projectile-target interaction are treated in the framework of perturbation theory. In Ref.[1] the laser-atom interaction is described by first order perturbation theory.

It is the aim of this paper to investigate free-free transitions in a bichromatic field that is the superposition of the fundamental and of the first harmonic at *moderate* field intensities for *fast* projectile. We are interested by this process in the case of atomic hydrogen in the ground state for frequencies which are large enough to produce important dressing effects. Section 2 is devoted to the approach adopted in this work; the formalism used by Varró and Ehlotzky [1] is extended: the description of the target dressing is improved by including second order corrections in the electromagnetic field. In Section 3 we discuss in detail the domain of small scattering angles showing that, in the limit of small momentum transfer and as long as the field intensities remain moderate, the nonperturbative approach that we use here reduces to a perturbative one. In the case of the considered bichromatic field we claim

that our calculations, which include second-order corrections to the atomic state, allow us to describe for each of the first four pairs of sidebands at least the leading process consistently (taking into account all the involved Feynman diagrams). Section 4 contains the numerical results obtained for fast projectile, E_i=100 eV, and two values of the fundamental frequency, namely $\omega = 1.17$ eV and $\omega = 4$ eV. Angular distributions and phase effects are discussed for different intensities in the moderate regime pointing out the role played by the second order dressing of the target.

II. BASIC FORMULA

This work is based on the assumption that at moderate field intensities (significantly lower than the atomic unit), the field-atom interaction can be described using time-dependent perturbation theory [9]. We use *second order* perturbation theory to describe the hydrogen ground state in the presence of the bichromatic field

$$\vec{\mathcal{A}}(t) = \vec{A}_1 \cos\omega_1 t + \vec{A}_2 \cos(2\omega_1 t + \varphi), \tag{1}$$

which is the superposition of the fundamental, of frequency ω_1, and of the first harmonic, of frequency $\omega_2 = 2\omega_1$. $\vec{A}_k = \vec{\varepsilon}_k\sqrt{I_k}/\omega_k$ is the vector potential of the component k, with $k = 1, 2$. $\vec{\varepsilon}_k$ denotes the polarization vector and I_k the intensity of that component, φ is the phase difference between the two components.

According to Florescu *et al* [10], one can write an approximate solution for a Coulomb electron in an electromagnetic field as follows

$$|\Psi_1(t)> = e^{-i\mathrm{E}_{1s}t}\left[|\psi_{1s}> + |\psi_{1s}^{(1)}> + |\psi_{1s}^{(2)}>\right], \tag{2}$$

where $|\psi_{1s}>$ is the unperturbed ground state of hydrogen, of energy E_{1s}, and $|\psi_{1s}^{(1,2)}>$ denote first and second order corrections, respectively. In agreement with Refs.[10] and [11] these corrections can be written in terms of the linear response

$$|\vec{w}_{1s}(\Omega)> = -G_C(\Omega)\vec{P}|\psi_{1s}>, \tag{3}$$

and of the second order tensor

$$|w_{ij,1s}(\Omega', \Omega)> = G_C(\Omega')P_i G_C(\Omega)P_j|\psi_{1s}>. \tag{4}$$

Here $G_C(\Omega)$ is the Coulomb Green's function and $\vec{P}$ is the momentum operator of the bound electron. For the bichromatic field (1), there are twelve values of the parameter of the Green functions which are necessary in order to write the approximate solution (2), namely

$$\Omega^{\pm} = \mathrm{E}_{1s} \pm (\omega_1 - \omega_2), \qquad \Omega'^{\pm} = \mathrm{E}_{1s} \pm (\omega_1 + \omega_2), \tag{5}$$

$$\Omega_k^{\pm} = \mathrm{E}_{1s} \pm \omega_k, \qquad \Omega_k'^{\pm} = \mathrm{E}_{1s} \pm 2\omega_k. \tag{6}$$

On the other hand, the interaction between the bichromatic field and the projectile is treated exactly by using the Volkov-type solution

$$\begin{aligned} \chi_{\vec{p}}(\vec{r},t) \;=\; & \frac{1}{(2\pi)^3} \exp\{-iE_p t + i\vec{p}\cdot\vec{r} \\ & -i\vec{p}\cdot[\vec{\alpha}_1(t) + \vec{\alpha}_2(t)]\}\,. \end{aligned} \tag{7}$$

where

$$\begin{aligned} \vec{\alpha}_1(t) \;&=\; \vec{\varepsilon_1}\alpha_{01}\sin(\omega_1 t), \\ \vec{\alpha}_2(t) \;&=\; \vec{\varepsilon_2}\alpha_{02}\sin(\omega_2 t + \varphi). \end{aligned} \tag{8}$$

$\vec{r}$ is the position, $\vec{p}$ the momentum, and E_p the energy of the free electron; $\alpha_{0k} = \sqrt{I_k}/\omega_k^2$ denotes the amplitude of the quiver motion for the component k of the field (1).

We restrict ourselves to the domain of high scattering energies, where first Born approximation in the scattering potential may be reliable. Neglecting the exchange effects, we describe this interaction by the static potential, $V(r,R)$, and the scattering matrix element is given by

$$S_{if}^{B1} = -i\int_{-\infty}^{+\infty} dt < \chi_{\vec{p}_f}(t)\Psi_1(t)|V|\chi_{\vec{p}_i}(t)\Psi_1(t) >, \tag{9}$$

where Ψ_1 and $\chi_{\vec{p}_{i,f}}$ are written using Eqs.(2) and (7).

In the presence of the radiation field (1) the electron scattered on hydrogen may gain or loose an energy equal to $n\omega_1$, such that $E_f = E_i + n\omega_1 \equiv E_i + n_1\omega_1 + n_2\omega_2$, where $E_{i(f)}$ is the initial (final) energy of the projectile and n_k is the net number of photons ω_k exchanged (absorbed or emitted) by the colliding system and the k component of the field. The energy spectrum of the scattered electron consists therefore of the elastic line, corresponding to $n = 0$, and of a number of sidebands, each pair of sidebands corresponding to the same $|n|$. The differential cross section for any process in which the energy of the projectile is *modified* by $n\omega_1$ is written as

$$\frac{d\sigma(n)}{d\Omega} = (2\pi)^4 \frac{p_f(n)}{p_i}|T_{if}(n)|^2, \tag{10}$$

where the transition matrix element, related to the S-matrix (9), has the following general structure

$$T_{if}(n) = T_n^{(0)} + T_n^{(1)} + T_n^{(2)}. \tag{11}$$

The first term,

$$T_n^{(0)} = B_n(a_1, a_2, \varphi) < \psi_{1s}|F(\vec{q})|\psi_{1s} >, \tag{12}$$

might be seen as the equivalent of Bunkin-Fedorov formula for a bichromatic field [2]. In the previous equation $F(\vec{q})$ is the form factor operator

$$F(\vec{q}) = \frac{1}{2\pi^2 q^2}\left[\exp\left(i\vec{q}\cdot\vec{r}\right) - 1\right] \tag{13}$$

and $B_n(a_1, a_2, \varphi)$ are generalized Bessel functions

$$B_n(a_1, a_2, \varphi) = \sum_{n_2=-\infty}^{\infty} J_{n-2n_2}(a_1) J_{n_2}(a_2) e^{-in_2\varphi}; \tag{14}$$

$\vec{q}(n)$ is the momentum transfer of the projectile, $\vec{q}(n) = \vec{p}_i - \vec{p}_f(n)$ such that $p_f^2/2 = p_i^2/2 + n\omega_1$, and the arguments of the two Bessel functions are given by

$$a_k(n) = \alpha_{0k}\ \vec{\varepsilon}_k \cdot \vec{q}(n). \tag{15}$$

If the dressing of the target is neglected then $T_{if}(n) = T_n^{(0)}$ and the generalized Bessel function, $B_n(a_1, a_2, \varphi)$, contains all the field dependence of the transition matrix in the same way in which $J_{n_1}(a_1)$ would do it in Bunkin-Fedorov formula [3] for a monochromatic field of frequency ω_1.

The other two terms in Eq.(11) are due to the modification of the atomic state in the bichromatic field. The second term, $T_n^{(1)}$, is connected to the first order corrections to the atomic state: one of the N photons exchanged between the field (1) and the colliding system interacts with the bound electron. We note that $N = |n_1| + |n_2| \neq n = n_1 + 2\ n_2$. This photon may have the energy ω_1 or ω_2, it may be emitted or absorbed, therefore the general structure of $T_n^{(1)}$ is given by

$$\begin{aligned} T_n^{(1)} \ = \ -\sum_{k=1}^{2} \frac{\alpha_{0k}\omega_k}{2} \Big[& B_{n+k}\ f_k^+(\varphi)\ \mathcal{M}_{at}^{(I)}\left(\Omega_k^-\right) \\ & + B_{n-k}\ f_k^-(\varphi)\ \mathcal{M}_{at}^{(I)}\left(\Omega_k^+\right)\Big], \end{aligned} \tag{16}$$

where $f_k^{\pm}$ is a function of the relative phase between the fields:

$$f_k^{\pm}(\varphi) = \begin{cases} 1 & \text{if } k{=}1 \\ \exp\left(\pm i\varphi\right) & \text{if } k{=}2. \end{cases} \tag{17}$$

$\mathcal{M}_{at}^{(I)}$ denotes the following matrix elements involving atomic states

$$\begin{aligned}\mathcal{M}_{at}^{(I)}\left(\Omega_k^{\pm}\right) &= <\psi_{1s}|F(\vec{q})|\vec{\varepsilon}_k\cdot\vec{w}_{1s}(\Omega_k^{\pm})> \\ &+ <\vec{\varepsilon}_k\cdot\vec{w}_{1s}(\Omega_k^{\mp})|F(\vec{q})|\psi_{1s}>, \end{aligned} \tag{18}$$

its significance will became clear in the next section.

Varró and Ehlotzky [1] studied free-free transitions in a bichromatic field taking into account only the first order corrections to the atomic ground state, the corresponding transition matrix element being given by the sum of $T_n^{(0)}$ and $T_n^{(1)}$. Moreover, in Ref.[1] the atomic matrix elements (18) were evaluated in the closure approximation. Very recently, some results were published [13], which are based on the Sturmian representation of the Coulomb Green's function.

Including second order corrections in the approximate description of the atomic ground state (2) we have to evaluate a third term, $T_n^{(2)}$, in Eq.(11). In this term two of the N photons exchanged between the fields and the colliding system interact with the bound electron:

$$\begin{aligned}T_n^{(2)} = \sum_{k=1}^{2}\frac{\alpha_{0k}^2\omega_k^2}{4}\Big\{ & B_{n+2k}\left[f_k^+(\varphi)\right]^2\mathcal{M}_{at}^{(II)}\left(\Omega_k'^-,\Omega_k^-\right) \\ & +B_{n-2k}\left[f_k^-(\varphi)\right]^2\mathcal{M}_{at}^{(II)}\left(\Omega_k'^+,\Omega_k^+\right) \\ & +B_n\left[\widetilde{\mathcal{M}}_{at}^{(II)}\left(\mathrm{E}_{1s},\Omega_k^-\right)+\widetilde{\mathcal{M}}_{at}^{(II)}\left(\mathrm{E}_{1s},\Omega_k^+\right)\right]\Big\} \\ +\frac{\alpha_{01}\alpha_{02}\omega_1\omega_2}{4}\Big[& B_{n+3}\,f_2^+(\varphi)\,\mathcal{N}_{at}^{(II)}\left(\Omega'^-,\Omega_1^-,\Omega_2^-\right) \\ & +B_{n-3}\,f_2^-(\varphi)\,\mathcal{N}_{at}^{(II)}\left(\Omega'^+,\Omega_1^+,\Omega_2^+\right) \\ & +B_{n+1}\,f_2^+(\varphi)\,\mathcal{N}_{at}^{(II)}\left(\Omega^+,\Omega_1^+,\Omega_2^-\right) \\ & +B_{n-1}\,f_2^-(\varphi)\,\mathcal{N}_{at}^{(II)}\left(\Omega^-,\Omega_1^-,\Omega_2^+\right)\Big]. \end{aligned} \tag{19}$$

Two types of atomic matrix elements appear in Eq.(19); they are related to the exchange of *identical* photons

$$\begin{aligned}&\mathcal{M}_{at}^{(II)}\left(\Omega_k'^{\pm},\Omega_k^{\pm}\right) = \\ &\sum_{j,l=1}^{3}\varepsilon_{kj}\varepsilon_{kl}\Big[<\psi_{1s}|F(\vec{q})|w_{lj,1s}\left(\Omega_k'^{\pm},\Omega_k^{\pm}\right)> \\ &\qquad + <w_{j,1s}(\Omega_k^{\mp})|F(\vec{q})|w_{l,1s}(\Omega_k^{\pm})> \\ &\qquad + <w_{lj,1s}\left(\Omega_k'^{\mp},\Omega_k^{\mp}\right)|F(\vec{q})|\psi_{1s}>\Big], \end{aligned} \tag{20}$$

or of *different* photons

$$\mathcal{N}_{at}^{(II)}\left(\tilde{\Omega}^{\pm},\Omega_m^{\pm},\Omega_n^{\pm}\right)=(1+\mathcal{P}_{mn})$$
$$\times\sum_{j,l=1}^{3}\varepsilon_{mj}\varepsilon_{nl}\Big[<\psi_{1s}|F(\vec{q})|w_{lj,1s}\left(\tilde{\Omega}^{\pm},\Omega_m^{\pm}\right)>$$
$$+<w_{j,1s}(\Omega_m^{\mp})|F(\vec{q})|w_{l,1s}(\Omega_n^{\pm})>$$
$$+<w_{lj,1s}\left(\tilde{\Omega}^{\mp},\Omega_m^{\mp}\right)|F(\vec{q})|\psi_{1s}>\Big], \tag{21}$$

where k, m, and n take the values 1 and 2, but $m \neq n$. $\tilde{\Omega}^{\pm}$ is a generic notation for $\Omega^{\pm}$ or $\Omega'^{\pm}$ defined in Eq.(5). $\mathcal{P}_{mn}$ denotes a permutation operator that interchanges the subscripts m and n. $\widetilde{\mathcal{M}}_{at}^{(II)}$ is built from Eq.(20) using the tensor $\widetilde{w}_{ij,1s}$, defined in Ref.[10], instead of $w_{ij,1s}$. For the sake of simplicity, the arguments of the generalized Bessel functions $B_n\left(a_1,a_2,\varphi\right)$ are omitted in Eqs.(16,19) as well as the q-dependence of the atomic matrix elements in Eqs.(18, 20-21). Different methods may be used to evaluate the atomic matrix elements in Eqs.(18, 20-21), which are already known from perturbative calculations involving one [6],[12] or two photons [7],[8]. We use in the numerical evaluations reported here the analytic expressions of these atomic matrix elements as series of hypergeometric functions [8],[12].

III. SMALL SCATTERING ANGLES

For small values of the arguments a_1 and a_2, the Bessel functions $J_{n_1}\left(a_1\right)$ and $J_{n_2}\left(a_2\right)$ have approximate values given by

$$J_n(x)\simeq\frac{1}{n!}\left(\frac{x}{2}\right)^n \tag{22}$$

and the generalized Bessel functions, $B_n(a_1,a_2,\varphi)$, can be approximated by a sum of a few terms, as it is shown below. In general, the arguments a_1 and a_2 are small for low field intensities where one recovers perturbative results. It is important to note that, in those geometries for which the polarization vector is almost orthogonal to the momentum transfer of the projectile, these arguments are small for every intensity since $a_{1,2}\sim\vec{\varepsilon}_{1,2}\cdot\vec{q}$.

We focus here the attention on the case of linear, identical polarizations $\vec{\varepsilon}_1=\vec{\varepsilon}_2\equiv\vec{\varepsilon}$, for the geometry in which the initial momentum is parallel to the polarization vector, defining the Oz-axis. Based on the previous remark, we show that in this geometry, for small scattering angles such that $\vec{\varepsilon}\cdot\vec{q}\ll 1$ and as long as the intensities remain moderate,

perturbation theory might represent a sensible treatment of free-free transitions. For the bichromatic field (1) the approach developed here allows us to study the leading processes to the first four pairs of sidebands, $|n| \leq 4$ in Eq.(10). In addition, for the first two pairs of sidebands, the first high order processes are also taken into account. In all these cases, all the involved Feynman diagrams are included, enabling us to account consistently for the effects of the target dressing. We remind that in this geometry the dressing of the target, connected to the last two terms in Eq.(11), is important at small scattering angles. For large scattering angles $a_{1,2}$ might be large and perturbation theory may no longer be valid if the fields are high enough. The dressing of the target is negligible for large scattering angles therefore the dominant contribution comes from the electronic diagrams, related to the term $T_n^{(0)}$; no significant differences between results based on Eq.(11) and Ref.[2] are to be expected in this domain.

A. First pair of sidebands: $n = \pm 1$

To prove that, in the geometry chosen here, perturbation theory is a reliable treatment at small scattering angles let us see what is the behavior of the transition matrix element (11) in the limit $a_{1,2} \ll 1$. The key point in this analysis is the behavior of the generalized Bessel functions (14) when use is made of Eq.(22). Our goal is to describe consistently at least the leading contribution to each sideband with $|n| \leq 4$, therefore we keep systematically second order terms in the fields. To fulfill the same goal for higher $|n|$ it would be necessary to add higher order corrections to the atomic state (2).

For $n = 1$ we discuss in some detail each of the three terms in Eq.(11). Keeping only second order contributions in the fields, one has

$$\begin{aligned} B_1\left(a_1, a_2, \varphi\right) &\simeq J_1(a_1)J_0(a_2) + J_{-1}(a_1)J_1(a_2)e^{-i\varphi} \\ &\simeq \frac{a_1}{2} - \frac{a_1 a_2}{4}e^{-i\varphi}, \end{aligned} \tag{23}$$

which leads to the following form of the electronic term

$$T_1^{(0)} \simeq \left(\frac{a_1}{2} - \frac{a_1 a_2}{4}e^{-i\varphi}\right) < \psi_{1s}|F(\vec{q})|\psi_{1s} > . \tag{24}$$

In this equation we neglect all the terms of order three or higher, namely $a_1^j a_2^{s-j}$ with $s \geq 3$ and $j = \overline{0, s}$. Each of the two terms in Eq.(24) is connected to a specific quantum path. In

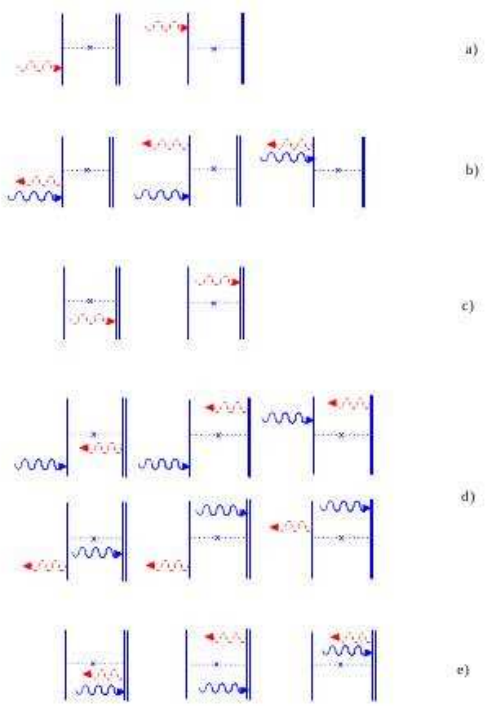

FIG. 1: (a) Feynman diagrams corresponding to one photon absorption by the projectile. The single line represents the free- and the double one the bound-electron. The horizontal line denotes the projectile-target interaction. (b) Feynman diagrams describing the absorption of ω_2 and the emission of ω_1 by the free electron. (c) Same as Fig.1(a) but for the bound electron. (d) Feynman diagrams in which each electron interacts with one photon. (e) Same as Fig.1(b) but for the bound electron.

the first one the projectile absorbs one photon of energy ω_1. It is described by two Feynman diagrams shown in Fig.1(a). In the second term the projectile absorbs a photon of energy $\omega_2 = 2\omega_1$ and emits a photon of energy ω_1, the scattered electron has the same final energy as in the previous case: $E_f = E_i + \omega_1$. This term is of the second order in the fields and it is described by six Feynman diagrams. Only three of them are shown in Fig.1(b), the other three are obtained by interchanging ω_1 and ω_2 in time (interchanging their order on the vertical lines).

A similar technique is used to find out the behavior of the second term in Eq.(11). In the limit we are interested in, only three generalized Bessel functions have a contribution to Eq.(16), namely B_0, B_{-1}, and B_2. The fourth one, B_3, has a leading term which is of higher

order in the fields, therefore it is neglected. Finally, one gets

$$T_1^{(1)} \simeq -\frac{1}{2}\left\{\alpha_{01}\omega_1 \mathcal{M}_{at}^{(I)}\left(\Omega_1^+\right)\right. \tag{25}$$
$$\left. + \alpha_{01}\alpha_{02}\frac{\vec{\varepsilon}\cdot\vec{q}}{2}e^{-i\varphi}\left[\omega_1 \mathcal{M}_{at}^{(I)}\left(\Omega_1^-\right) - \omega_2 \mathcal{M}_{at}^{(I)}\left(\Omega_2^+\right)\right]\right\}.$$

The first term involves one photon ω_1 that is absorbed by the atomic electron. The corresponding two Feynman diagrams can be seen in Fig.1(c). The second term involves two photons of different colors: a photon ω_1 is emitted by the bound/free electron and an other photon, ω_2, is absorbed by the free/bound electron. In Fig.1(d) only six Feynman diagrams are shown, the other six are obtained by interchanging in time ω_1 and ω_2.

In the limit $a_{1,2} \ll 1$, the last term in Eq.(11) has only one contribution, given by the last line in Eq.(19)

$$T_1^{(2)} \simeq \frac{1}{4}\alpha_{01}\alpha_{02}\omega_1\omega_2\, e^{-i\varphi}\, \mathcal{N}_{at}^{(II)}\left(\Omega^-, \Omega_1^-, \Omega_2^+\right). \tag{26}$$

It represents a second order term in which both photons, ω_1 and ω_2, interact with the atomic electron. Three of the six corresponding Feynman diagrams are shown in Fig.1(e).

Adding together the approximate forms in Eqs.(24-26), one gets finally the following form of the transition matrix element

$$\begin{aligned} T(1) \;\simeq\; & \frac{\alpha_{01}}{2}\left[\vec{\varepsilon}\cdot\vec{q} < \psi_{1s}|F(\vec{q})|\psi_{1s} > -\omega_1 \mathcal{M}_{at}^{(I)}\left(\Omega_1^+\right)\right] \\ & + \; e^{-i\varphi}\,\frac{\alpha_{01}\alpha_{02}}{4}\left\{-\left(\vec{\varepsilon}\cdot\vec{q}\right)^2 < \psi_{1s}|F(\vec{q})|\psi_{1s} > \right. \\ & \qquad + \vec{\varepsilon}\cdot\vec{q}\,\left[\omega_2 \mathcal{M}_{at}^{(I)}\left(\Omega_2^+\right) - \omega_1 \mathcal{M}_{at}^{(I)}\left(\Omega_1^-\right)\right] \\ & \qquad \left. + \omega_1\omega_2 \mathcal{N}_{at}^{(II)}\left(\Omega^-, \Omega_1^-, \Omega_2^+\right)\right\}. \end{aligned} \tag{27}$$

The first **line** in this equation represents the transition matrix element, denoted by T_a, describing one photon absorption (see Fig.2(a) and the corresponding Feynman diagrams in Figs.1(a) and (c)). The remaining part, T_b, describes the two photon process shown in Fig. 2(b) (see also Figs.1(b), (d) and (f)).

Accordingly, the differential cross section for the process in which the scattered projectile has the energy $E_f = E_i + \omega_1$ is approximated at small scattering angles by

$$\begin{aligned} \frac{d\sigma(1)}{d\Omega} \;\simeq\; & (2\pi)^4 \frac{p_f}{p_i} I_1 \left[|\mathcal{T}_a|^2 + I_2|\mathcal{T}_b|^2 \right. \\ & \left. + 2\sqrt{I_2}\; Re\left(\mathcal{T}_a^* \mathcal{T}_b e^{-i\varphi}\right)\right], \end{aligned} \tag{28}$$

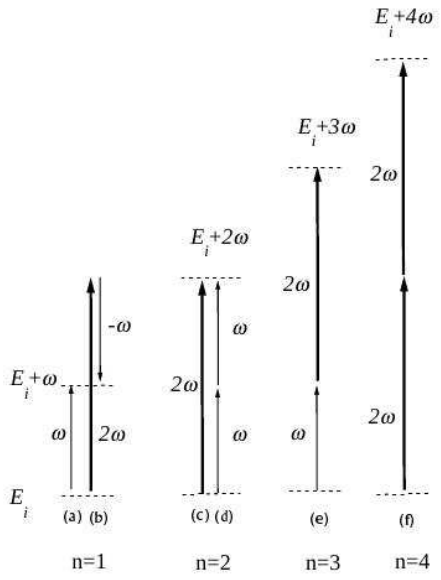

FIG. 2: **(a-b)** Channels leading to the final energy $E_f = E_i + n\omega_1$ with $n = 1$. **(c-d)** Same as Fig.2(a) but $n = 2$. **(e)** Same as Fig.2(a) but $n = 3$. **(f)** Same as Fig.2(a) but $n = 4$.

where we have chosen to display explicitly the dependence of the transition matrix elements on the intensities and on the relative phase of the fields: $T_a \equiv \sqrt{I_1}\mathcal{T}_a$ and $T_b \equiv \sqrt{I_1 I_2}\mathcal{T}_b\, e^{-i\varphi}$.

The same techniques may be used to study the case $n = -1$, where the final energy is $E_f = E_i - \omega_1$ and the dominant process is the stimulated emission of a photon ω_1.

B. Other sidebands: $n = \pm 2,\ \pm 3,\ \pm 4$

The procedure presented before is now applied for the next sideband, $n = 2$. In this case the scattered electrons have the energy $E_f = E_i + 2\omega_1$. In the limit $a_{1,2} \ll 1$, keeping again only second order terms in the fields, the approximate transition matrix element has a form similar to that given in Eq.(27), namely

$$\begin{aligned} T(2) \;\simeq\; & e^{-i\varphi}\frac{\alpha_{02}}{2}\left[\vec{\varepsilon}\cdot\vec{q} < \psi_{1s}|F(\vec{q})|\psi_{1s} > -\omega_2 \mathcal{M}_{at}^{(I)}\left(\Omega_2^+\right)\right] \\ + \;& \frac{\alpha_{01}^2}{4}\left[\frac{1}{2}\left(\vec{\varepsilon}\cdot\vec{q}\right)^2 < \psi_{1s}|F(\vec{q})|\psi_{1s} > \right. \\ - \;& \left.\vec{\varepsilon}\cdot\vec{q}\,\omega_1 \mathcal{M}_{at}^{(I)}\left(\Omega_1^+\right) + \omega_1^2 \mathcal{M}_{at}^{(II)}\left(\Omega_1'^+, \Omega_1^+\right)\right]. \end{aligned} \tag{29}$$

The first **line** represents the transition matrix element describing the absorption of one photon ω_2 in Fig.2(c) and it is denoted by T_c. The remaining part, denoted by T_d, describes

the absorption of two photons ω_1, shown in Fig. 2(d).

The differential cross section for the process in which the scattered projectile has the energy $E_f = E_i + 2\omega_1$ is approximated at small scattering angles by

$$\frac{d\sigma(2)}{d\Omega} \simeq (2\pi)^4 \frac{p_f}{p_i} I_2 \left[|\mathcal{T}_c|^2 + \frac{I_2}{\mathrm{f}^2} |\mathcal{T}_d|^2 + 2\frac{\sqrt{I_2}}{\mathrm{f}} Re\left(\mathcal{T}_c^* \mathcal{T}_d e^{-i\varphi}\right)\right], \tag{30}$$

where we display again the explicit dependence on the intensities and phase: $T_c \equiv \sqrt{I_2}\mathcal{T}_c$ and $T_d \equiv I_1 \mathcal{T}_d \, e^{-i\varphi}$. f denotes in Eq.(30) the ratio between the intensities of the harmonic and the fundamental, $\mathrm{f} = I_2/I_1$.

When the limit $a_{1,2} \ll 1$ is taken for $n = 3$ and $n = 4$ in Eq.(11), one gets:

$$\begin{aligned} T(3) \simeq\ & e^{-i\varphi} \frac{\alpha_{01}\alpha_{02}}{4} \Big\{ (\vec{\varepsilon}\cdot\vec{q})^2 < \psi_{1s}|F(\vec{q})|\psi_{1s} > \\ & -\vec{\varepsilon}\cdot\vec{q}\left[\omega_1 \mathcal{M}_{at}^{(I)}\left(\Omega_1^+\right) + \omega_2 \mathcal{M}_{at}^{(I)}\left(\Omega_2^+\right)\right] \\ & + \omega_1\omega_2 \mathcal{N}_{at}^{(II)}\left(\Omega'^+, \Omega_1^+, \Omega_2^+\right)\Big\} \end{aligned} \tag{31}$$

and

$$\begin{aligned} T(4) \simeq\ & e^{-2i\varphi} \frac{\alpha_{02}^2}{4} \left[\frac{1}{2}(\vec{\varepsilon}\cdot\vec{q})^2 < \psi_{1s}|F(\vec{q})|\psi_{1s} > \right. \\ & \left. -\ \vec{\varepsilon}\cdot\vec{q}\,\omega_2 \mathcal{M}_{at}^{(I)}\left(\Omega_2^+\right) + \omega_2^2 \mathcal{M}_{at}^{(II)}\left(\Omega_2'^+, \Omega_2^+\right)\right]. \end{aligned} \tag{32}$$

At small scattering angles, in the framework of the approach used here and as long as we restrict ourselves to the second order in the electric fields, the dominant process for $n = 3$ is the absorption of two photons of different colors (see Fig.2(e)). For $n = 4$, the dominant process is the absorption of two harmonic photons (see Fig.2(f)). In this approximation the differential cross sections have simpler dependences on the intensity of the fields:

$$\frac{d\sigma(3)}{d\Omega} \simeq (2\pi)^4 \frac{p_f}{p_i} I_1 I_2 |\mathcal{T}_e|^2, \tag{33}$$

$$\frac{d\sigma(4)}{d\Omega} \simeq (2\pi)^4 \frac{p_f}{p_i} I_2^2 |\mathcal{T}_f|^2. \tag{34}$$

The relative phase between the fields is not a relevant parameter if only the leading process is taken into account.

IV. NUMERICAL RESULTS AND DISCUSSION

We focus our attention on the study of free-free transitions in electron-hydrogen scattering in the presence of a bichromatic field for a high initial energy of the projectile, $E_i = 100$ eV. Its initial momentum, $\vec{p}_i$, is parallel to the polarization vectors of the fields, $\vec{\varepsilon}$, and defines the Oz-axis. We are interested in the differential cross sections for processes in which the energy of the scattered projectile is $E_f = E_i + n\omega_1$ with n an integer such that $-4 \leq n \leq 4,\ n \neq 0$. Having in mind the analysis presented in the previous section, we investigate in detail the domain of small scattering angles, where the dressing of the target is important. The effect of the intensities of the two components of the bichromatic field and that of their relative phase is investigated for two cases: $\omega = 1.17$ eV and $\omega = 4$ eV.

A. $\omega = 1.17$ eV

Figs.3(a-d) show the differential cross sections calculated for a bichromatic field that is the superposition of the fundamental and the first harmonic of Nd:YAG laser (ω_1=1.17 eV). We treat here the case of equal intensities, $I_1 = I_2 = 10^{12}$ W/cm^2, and we consider that the fields are in phase, $\varphi = 0$. Full lines are used to represent the differential cross sections calculated when all three terms are included in Eq.(11) and Eqs.(12), (16), and (19) are used to compute them. For $n = \pm 1; \pm 2$ the dominant process is of the first order in the field, the frequency of the absorbed/emitted photon is ω_1 when $n = \pm 1$ and ω_2 when $n = \pm 2$. At this intensity, the interferences due to second order processes (Figs.2(b) and (d)) are negligible; they do not play any significant role below $I_{1,2} = 10^{13}$ W/cm^2. For $|n| \geq 3$ the dominant process involves two photons (see Fig.2(e) and (f)). In general, no significant deviations from the perturbative regime exist in Figs.3 when $\theta < 20^0$. The case $n = -4$ is an exception: the minimum at $\theta = 16^0$ is due to the interference between the terms in Eq.(11), it is located close to a zero of $B_{-4}(a_1, a_2, 0)$.

We note that in the forward direction the differential cross sections are comparable for first order processes, $n = \pm 1$ and ± 2; for second order processes, $n = \pm 3$ and ± 4, they are at least three orders of magnitude smaller.

Also displayed in these figures are the results based on the first order dressing of the target. This approximation implies that the transition matrix element in Eq.(11) contains

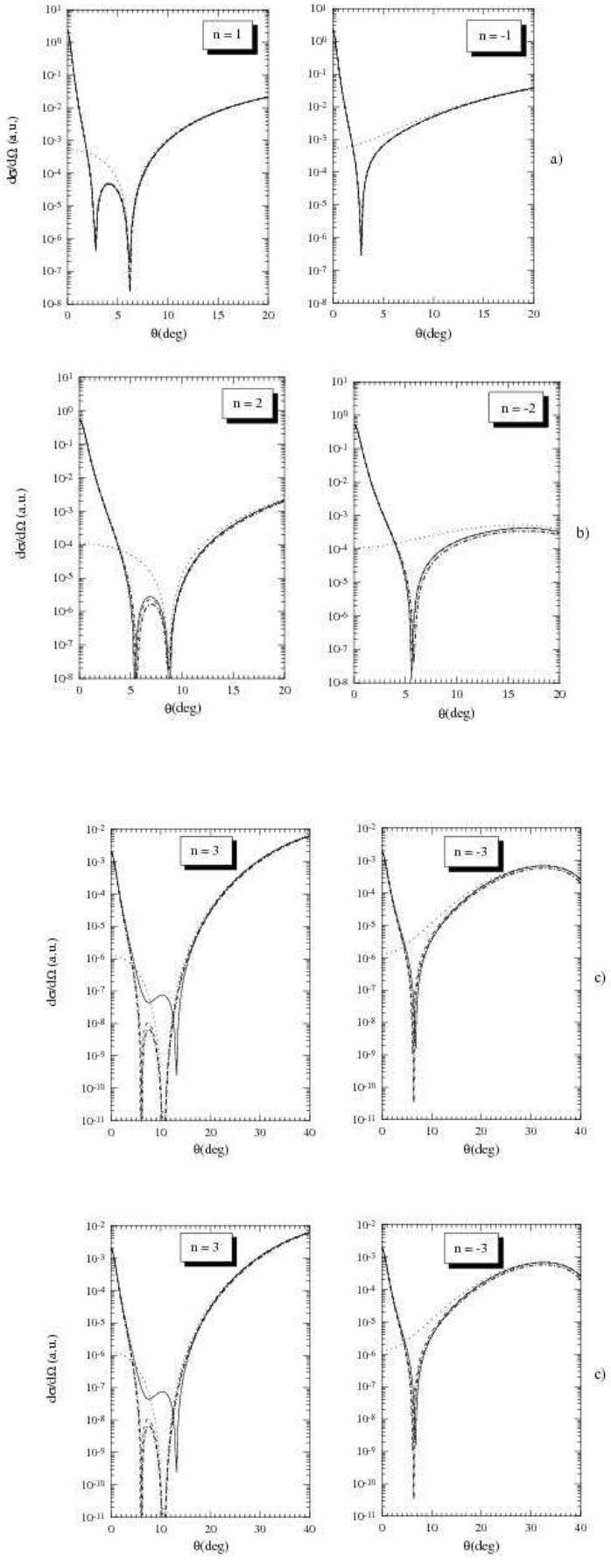

FIG. 3: **(a)** Differential cross sections for $|n| = 1$ as a function of the scattering angle θ at the

only the first two terms. By inspecting Figs.3 one can see that this approximation (dashed line) is very good for $|n| \leq 2$, but it can not reproduce the minimum structure of the differential cross sections for $n = 3, 4$.

We note also that the closure approximation (dotted-dashed line) is excellent for $n = \pm 1$ and quite fair for $n = \pm 2$. As expected, the electronic contribution alone (dotted line) fails at small scattering angles.

We have also investigated the situation in which the two components of the bichromatic field have different intensities. We have chosen to illustrate the intensity dependence of the angular distribution for the second pair of sidebands, $n = \pm 2$. In Fig.4 three different values of the harmonic intensity are considered but the intensity of the fundamental is the same, $I_1 = 10^{13}\mathrm{W/cm^2}$. The harmonic intensities correspond to three values of the ratio $\mathrm{f} = \mathrm{I_2/I_1}$, namely f=1 represented by full lines, f =0.1 by dotted-dashed lines, and f =0.01 by dotted lines.

In Fig.4(a) the field components are in phase, $\varphi = 0$, and in Fig.4(b) they are out of phase, $\varphi = \pi$. The interferences effects are significant for small values of f, as can be understood from Eq.(30), because in this case the second order processes are due to fields which are much stronger than the harmonic field that gives first order processes. Comparing the graphs in Figs.4(a) and (b) one can see the effect of the relative phase, too.

Figs.5 display the φ-dependence of the laser assisted signal for $n = 2$ at two scattering angles: $\theta = 2^0$ in Fig.5(a) and $\theta = 7^0$ in Fig.5(b). The fundamental and the harmonic have the same intensities as in Fig.4. At $\theta = 2^0$ the laser assisted signals have their minimal value when the fields are in phase. The situation is different for $\theta = 7^0$: the signals decrease when the fields are out of phase. When the perturbative treatment is valid, for a fixed scattering angle, the difference between the laser assisted signals at $\varphi = 0$ and $\varphi = \pi$ is proportional to $4\sqrt{\mathrm{f}I_1^3}\mathcal{T}_c\mathcal{T}_d$ and decreases for weaker harmonic intensities. Nevertheless, as discussed earlier, the interference between first and second order processes is stronger in this case. The differential cross sections in Eqs.(28, 30) have different formal dependences on the intensities of the two components of the bichromatic field. This explains why the interferences between first and second order processes and the phase effects are both stronger for stronger harmonics when $n = \pm 1$. Note however that the interference effects are significantly affected whenever the frequencies match an atomic resonance.

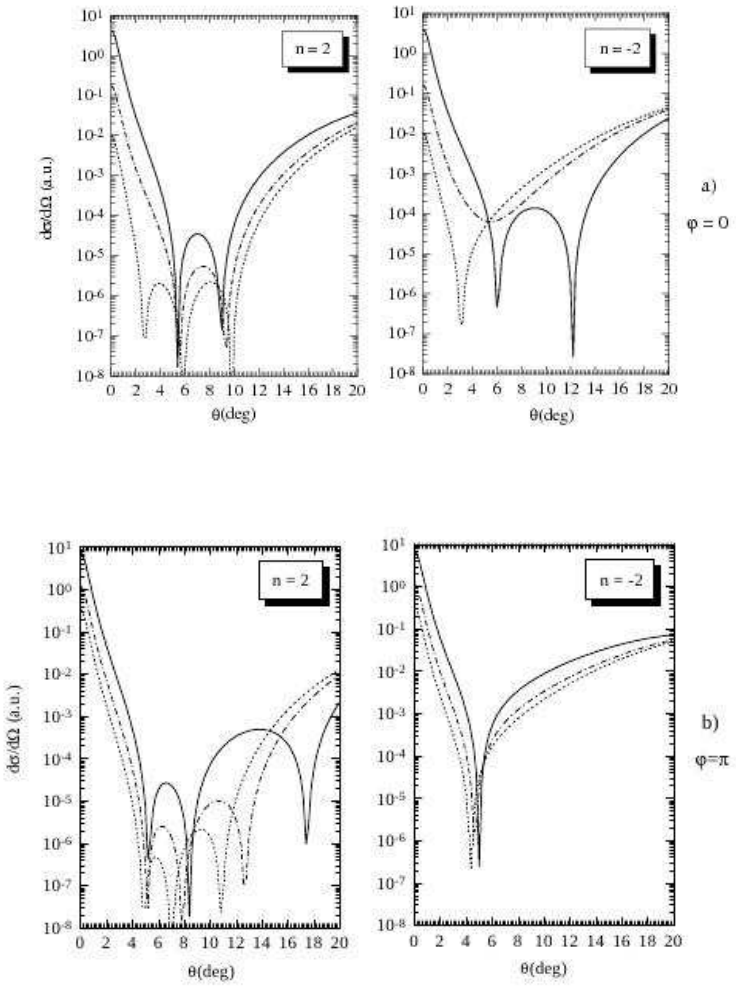

FIG. 4: **Fig.4(a)** Differential cross sections, based on Eq.(11), for $|n| = 2$ as a function of the scattering angle θ at the initial energy $E_i = 100$ eV for Nd:YAG laser. The intensity of the fundamental is $I_1 = 10^{13}$ W/cm^2 and the fields are in phase; the harmonic intensity corresponds to the following cases: f = 1 (full line), f = 0.1 (dotted-dashed line), and f = 0.01 (dotted line). **Fig.4(b)** Same as Fig.4(a) but $\varphi = \pi$.

B. $\omega = 4$ eV

Our interest for higher frequencies is due to the fact that, on one hand, the dressing of the target is more important than for low frequencies and, on the other hand, the quiver amplitude is smaller, which increases the θ-domain for which one can successfully apply the perturbation theory. Figs.6 show the differential cross sections for the first three pairs of sidebands, $|n| \leq 3$ at the fundamental frequency $\omega_1 = 4$ eV, when the field components are

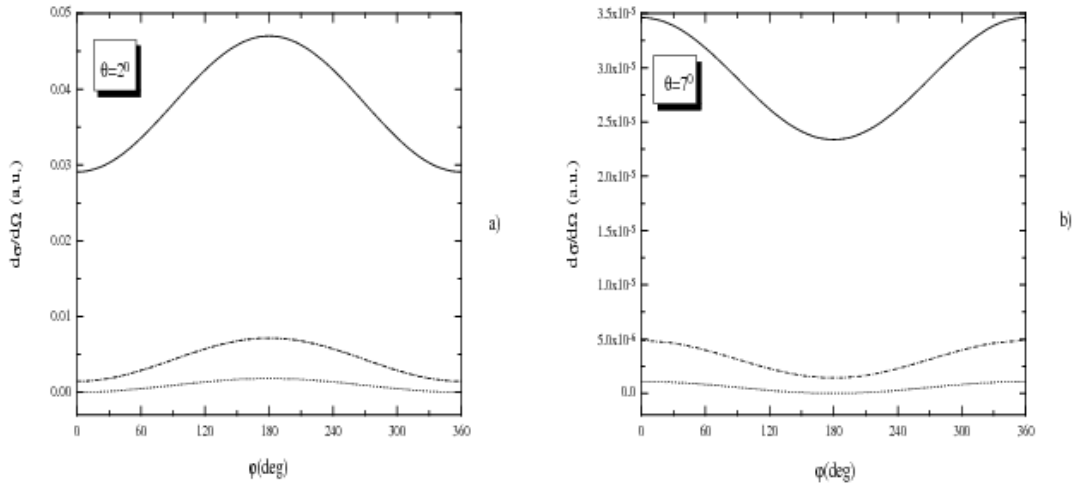

FIG. 5: **Fig.5(a)** Differential cross sections, based on Eq.(11), for $n = 2$ as a function of the relative phase φ at the scattering energy $E_i = 100$ eV for Nd:YAG laser. The scattering angle is $\theta = 2^0$ and the fields intensities are the same as in Fig.4. **Fig.5(b)** Same as Fig.5(a) but $\theta = 7^0$.

in phase, $\varphi = 0$. The other conditions, concerning the geometry, the scattering energy, and the intensities, are the same as in Figs.3. The graphs in Fig.6(a), corresponding to $n = \pm 1$, show that the approximation based on the first order atomic dressing (dashed line) is quite good in the forward direction ($\theta < 5^0$) even in the closure approximation (dotted-dashed line). On the contrary, for $n = \pm 2$, in Fig.6(b), the closure approximation fails to give fair results for $\theta > 15^0$, but the first order target dressing leads again to rather good results if the atomic matrix elements (18) are evaluated exactly. The situation is completely different for $n = \pm 3$: in Fig.6(c) the first order dressing gives results which are completely inadequate for scattering angles smaller than $\theta = 30^0$. In addition, at large scattering angles, the closure approximation significantly overestimates the matrix elements (18), which affects considerably the differential cross sections.

V. CONCLUSIONS

Our investigations of free-free transitions in a bichromatic field at moderate intensities show that calculations based on a perturbative description of the target in the field are very helpful. At low frequencies, first order corrections account for the major dressing effects. For those situation in which these corrections give reliable descriptions we investigate the validity

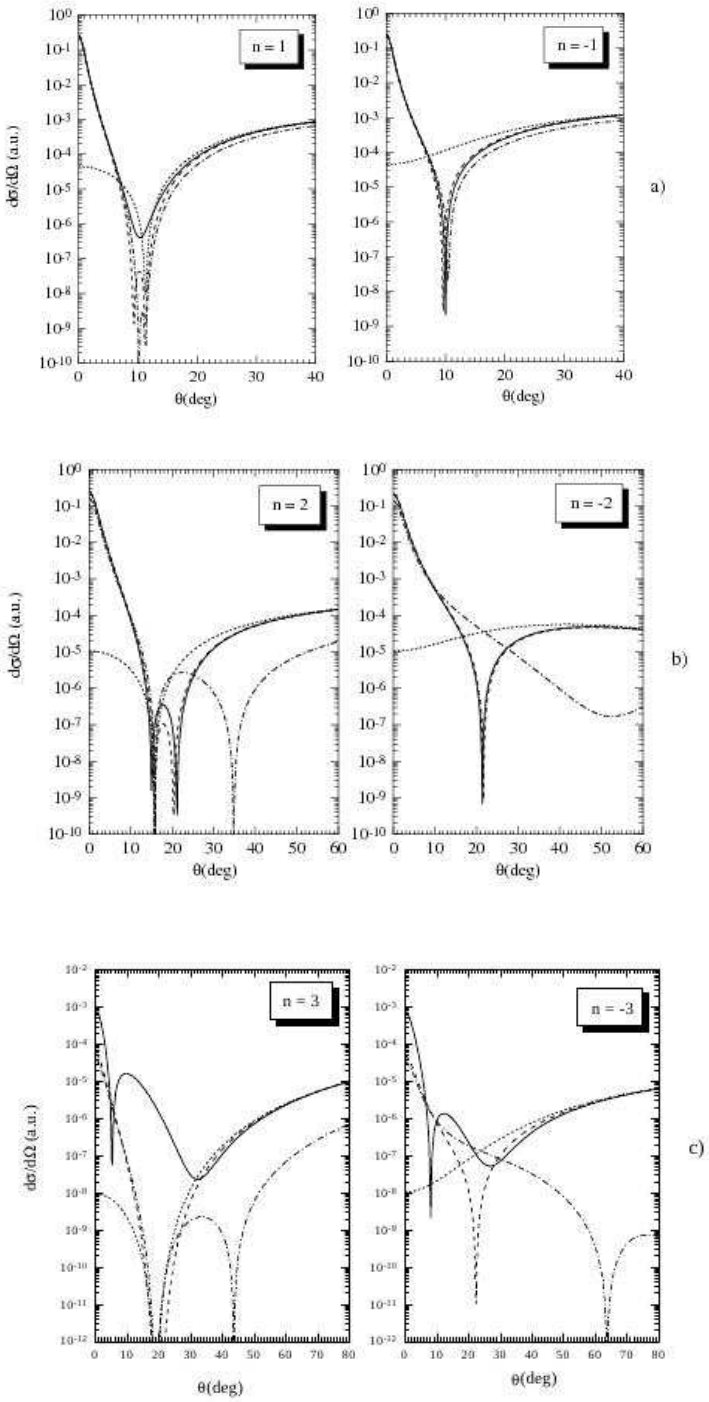

FIG. 6: **Fig.6(a-c)** Same as Fig.3(a-c) but $\omega_1 = 4$ eV.

of the closure approximation. We warn that its use should be limited to low frequencies and small scattering angles. We stress that, whenever the dominant process involves two photons, second order corrections are very important, especially at high frequencies. These corrections influence the angular distributions and the phase dependences of the laser assisted signals.

Acknowledgments

This research is supported in part by a Grant of the Romanian Ministry of Research.

---

[1] S. Varró and F. Ehlotzky, *J. Phys. B*, **30**, 1061 (1997)

[2] S. Varró and F. Ehlotzky, *Phys. Rev. A*, **47**, 715 (1993)

[3] F.V. Bunkin and M.V. Fedorov, *Zh. Eksp. Theor. Fiz.*, **49**, 1215 (1965)[1966, *Sov. Phys. JETP*, **22**, 884]

[4] F. Ehlotzky, *Nuovo Cimento D*, **16**, 453 (1994)

[5] N.M. Kroll and K.M. Watson, *Phys. Rev. A*, **8**, 804 (1973)

[6] A. Dubois, A. Maquet and S. Jetzke, *Phys. Rev. A*, **34**, 1888 (1986)

[7] G. Kracke, J.S. Briggs, A. Dubois, A. Maquet and V. Veniard, *J. Phys. B*, **27**, 3241 (1994)

[8] A. Cionga and G. Buică, *Laser. Phys.* **8**, 164 (1998)

[9] F.W. Byron Jr. and C.J. Joachain, *J. Phys. B*, **17**, L295 (1984)

[10] V. Florescu, A. Halasz, and M. Marinescu, *Phys. Rev. A*, **47**,394, (1993)

[11] V. Florescu and T. Marian, *Phys. Rev. A*, **34**, 4641 (1986)

[12] A. Cionga and V. Florescu, *Phys. Rev.A*, **45**, 5282 (1992)

[13] D. Milošević, F. Ehlotzky, and B. Piraux, *J. Phys. B*, **30**, 4347 (1997)

Figure Captions

Fig.1(a) Feynman diagrams corresponding to one photon absorption by the projectile. The single line represents the free- and the double one the bound-electron. The horizontal line denotes the projectile-target interaction. **Fig.1(b)** Feynman diagrams describing the absorption of ω_2 and the emission of ω_1 by the free electron. **Fig.1(c)** Same as Fig.1(a) but for the bound electron. **Fig.1(d)** Feynman diagrams in which each electron interacts with one photon. **Fig.1(e)** Same as Fig.1(b) but for the bound electron.

Fig.2(a-b) Channels leading to the final energy $E_f = E_i + n\omega_1$ with $n = 1$. **Fig.2(c-d)**

Same as Fig.2(a) but $n = 2$. **Fig.2(e)** Same as Fig.2(a) but $n = 3$. **Fig.2(f)** Same as Fig.2(a) but $n = 4$.

Fig.3(a) Differential cross sections for $|n| = 1$ as a function of the scattering angle θ at the initial energy $E_i = 100$ eV for Nd:YAG laser (ω_1=1.17 eV). $I_1 = I_2 = 10^{12}$ W/cm^2 and the fields are in phase, $\varphi = 0$. Full lines represent the results based on Eq.(11), dotted lines include only first order dressing, dotted-dashed lines correspond to the closure approximation, dotted lines do not include any dressing. **Fig.3(b)** Same as Fig.3(a) but $|n| = 2$. **Fig.3(c)** Same as Fig.3(a) but $|n| = 3$. **Fig.3(d)** Same as Fig.3(a) but $|n| = 4$.

Fig.4(a) Differential cross sections, based on Eq.(11), for $|n| = 2$ as a function of the scattering angle θ at the initial energy $E_i = 100$ eV for Nd:YAG laser. The intensity of the fundamental is $I_1 = 10^{13}$ W/cm^2 and the fields are in phase; the harmonic intensity corresponds to the following cases: f = 1 (full line), f = 0.1 (dotted-dashed line), and f = 0.01 (dotted line). **Fig.4(b)** Same as Fig.4(a) but $\varphi = \pi$.

Fig.5(a) Differential cross sections, based on Eq.(11), for $n = 2$ as a function of the relative phase φ at the scattering energy $E_i = 100$ eV for Nd:YAG laser. The scattering angle is $\theta = 2^0$ and the fields intensities are the same as in Fig.4. **Fig.5(b)** Same as Fig.5(a) but $\theta = 7^0$.

Fig.6(a-c) Same as Fig.3(a-c) but $\omega_1 = 4$ eV.

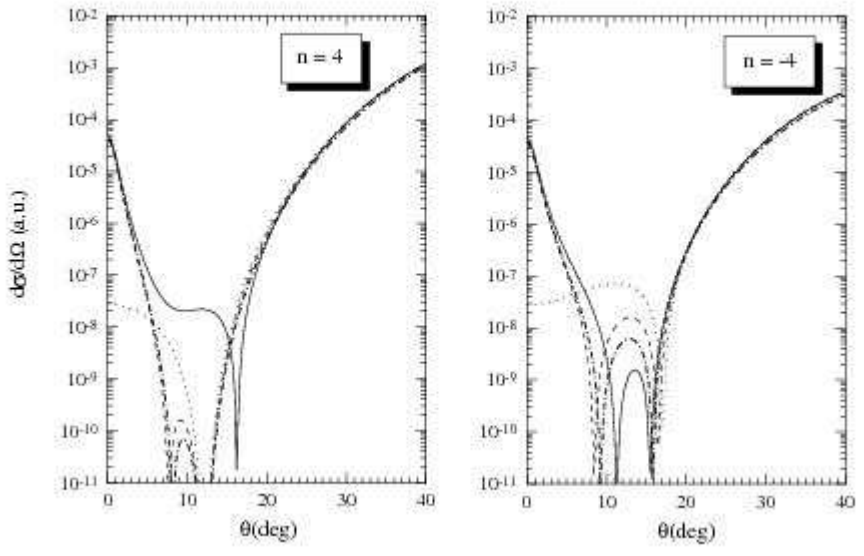

d)